ApJ ACCEPTED [30 MARCH 2004]
Preprint typeset using LaTeX style emulateapj v. 2/19/04

A POPULATION OF MASSIVE GLOBULAR CLUSTERS IN NGC 5128

PAUL MARTINI
Harvard-Smithsonian Center for Astrophysics; 60 Garden Street, MS20; Cambridge, MA 02138; pmartini@cfa.harvard.edu
AND
LUIS C. HO
Observatories of the Carnegie Institution of Washington; 813 Santa Barbara Street; Pasadena, CA 91101; lho@ociw.edu
ApJ accepted [30 March 2004]

ABSTRACT

We present velocity dispersion measurements of 14 globular clusters in NGC 5128 (Centarus A) obtained with the MIKE echelle spectrograph on the 6.5m Magellan Clay telescope. These clusters are among the most luminous globular clusters in NGC 5128 and have velocity dispersions comparable to the most massive clusters known in the Local Group, ranging from 10 – 30 km s^{-1}. We describe in detail our cross-correlation measurements, as well as simulations to quantify the uncertainties. These 14 globular clusters are the brightest NGC 5128 globular clusters with surface photometry and structural parameters measured from the *Hubble Space Telescope*. We have used these measurements to derive masses and mass-to-light ratios for all of these clusters and establish that the fundamental plane relations for globular clusters extend to an order of magnitude higher mass than in the Local Group. The mean mass-to-light ratio for the NGC 5128 clusters is $\sim 3 \pm 1$, higher than measurements for all but the most massive Local Group clusters. These massive clusters begin to bridge the mass gap between the most massive star clusters and the lowest-mass galaxies. We find that the properties of NGC 5128 globular clusters overlap quite well with the central properties of nucleated dwarf galaxies and ultracompact dwarf galaxies. As six of these clusters also show evidence for extratidal light, we hypothesize that at least some of these massive clusters are the nuclei of tidally stripped dwarfs.

Subject headings: galaxies: individual (NGC 5128) — galaxies: star clusters — globular clusters: general

1. INTRODUCTION

Globular clusters provide valuable snapshots of the formation history of galaxies and their large sizes and luminosities make them the most readily observable sub-galactic constituents. In addition, globular clusters exhibit surprisingly uniform properties that suggests a common formation mechanism. They are well-fit by single-mass, isotropic King models (King 1966), which describe clusters in terms of scale radii, central surface brightness, and core velocity dispersion. Detailed studies of globular clusters in our Galaxy have shown that in fact they only inhabit a narrow range of the parameter space available to King models (Djorgovski 1995; McLaughlin 2000) and other globular cluster systems in the Local Group also appear to approximately follow the same relations (Djorgovski et al. 1997; Dubath & Grillmair 1997; Dubath et al. 1997; Barmby et al. 2002; Larsen et al. 2002). These parameter correlations trace a globular cluster fundamental plane that is analogous to, but distinct from, the fundamental plane for elliptical galaxies (Dressler et al. 1987; Djorgovski & Davis 1987; Bender et al. 1992; Burstein et al. 1997).

Globular cluster studies that include internal kinematics have been confined to the Local Group due to the faint apparent magnitudes of more distant extragalactic globular clusters. These studies have therefore only included the globular cluster systems of spiral and dwarf galaxies and not the globular cluster systems of large ellipticals. Yet the globular cluster systems of ellipticals are a particularly interesting regime as they probe both a new morphological type and one likely to have exhibited a different and more complex formation history. The globular cluster systems of elliptical galaxies, as well as many spirals such as our own, have bimodal color distributions suggestive of multiple episodes of formation (e.g. Kundu & Whitmore 2001; Larsen et al. 2001). Models for the formation of these globular cluster systems posit that one of these populations may be the intrinsic population of the galaxy and subsequent mergers resulted in the second population either as the result of a new episode of globular cluster formation (Schweizer 1987; Ashman & Zepf 1992; Forbes, Brodie, & Grillmair 1997) or accretion of globular cluster systems from other galaxies, including accretion of globular clusters by tidal stripping from other members of a cluster of galaxies (Côté, Marzke, & West 1998).

NGC 5128 (Centarus A), as the nearest large elliptical galaxy, is arguably the best source for extending detailed globular cluster studies outside of the Local Group. While NGC 5128 is the central galaxy of a large group, rather than a giant elliptical in a cluster, it likely had a similar formation history to its larger cousins. The most relevant similarity is the strong evidence for a recent, gas-rich merger (for a recent review of NGC 5128 see Israel 1998). Estimates of the size of the NGC 5128 globular cluster population suggest that it has a total of ~ 2000 clusters, approximately a factor of 3 more than the entire Local Group (Harris et al. 1984). Simple scaling arguments suggest that NGC 5128 should possess a number of extremely massive globular clusters and therefore is not only a good target for study of the globular cluster system of an elliptical galaxy, but also for study of how well the fundamental plane relations established locally apply to more massive globular clusters. A recent photometric and spectroscopic study of NGC 5128 by Peng, Ford, & Freeman (2004a,b) concluded that the metal-rich globular clusters may have a mean age of 5^{+3}_{-2} Gyr, while an analysis of their photometric data yields a metallicity range of –2.0 through +0.3 (Yi et al. 2004)

The most massive globular clusters can also be used to explore connections between the formation processes for star clusters and galaxies. While fundamental plane studies (e.g.

Burstein et al. 1997) clearly illustrate a significant mass gap between the most massive Galactic globular clusters and the least massive dwarf galaxies, there have been encroachments into this gap from both sides. For many years, studies have speculated that at least some globular clusters may be the remains of tidally-stripped dwarf galaxy nuclei (Zinnecker et al. 1988; Freeman 1993; Bassino et al. 1994). Two of the most massive globular clusters in the Local Group, ωCen in our Galaxy and G1 in M31, have been interpreted as the nuclei of tidally stripped dwarfs (Meylan et al. 2001; Gnedin et al. 2002; Bekki & Freeman 2003). From the galaxy side, recent studies of nucleated dwarf galaxies in the Virgo cluster (Geha, Guhathakurta, & van der Marel 2002) and ultracompact dwarf galaxies in the Fornax cluster (Drinkwater et al. 2003) show some similarities between these least-massive galaxies and the most massive globular clusters. This mass gap may thus reflect the scarcity of the most massive globular clusters and the difficulty of kinematic measurements for the least massive, lowest surface-brightness dwarf galaxies, rather than a physical separation.

In this paper we present velocity dispersion measurements for 14 globular clusters in NGC 5128. These globular clusters were selected from the *Hubble Space Telescope* (*HST*) study of Harris et al. (2002) and therefore have well-measured structural parameters. These data are combined to estimate masses for these clusters, masses that are among the largest known for any star clusters and comparable to the nuclei of the lowest-mass galaxies. In the next sections we describe the observations, data processing, and velocity dispersion measurements. Analysis of these measurements is described in §5 and the potential link between star clusters and galaxies is explored in §6. Our results are summarized in the final section. Throughout this paper we adopt the distance of 3.84 ± 0.35 Mpc for NGC 5128 determined by Rejkuba (2004) from the brightness of the tip of the red giant branch and the Mira period-luminosity relation.

2. OBSERVATIONS

Spectra of 14 globular clusters in NGC 5128 were obtained in the course of seven nights in March 2003 with the MIKE echelle spectrograph (Bernstein et al. 2003) and the 6.5m Magellan Clay telescope at Las Campanas Observatory (see Table 1). MIKE is a double echelle spectrograph capable of resolution $R = 19,000$ on the red side when used with the $1''$ slit selected for these observations. This corresponds to a velocity resolution FWHM of 15.8 km s^{-1} or σ = 6.2 km s^{-1}. MIKE was located at the East Nasmyth port but not directly attached to the instrument rotator. The advantage of this configuration is that the instrument is gravity invariant and therefore potential calibration difficulties due to instrument flexure are completely avoided. The disadvantage of this configuration is that targets could not be observed at the parallactic angle and that they rotate with respect to the spectrograph slit. In any event, this configuration was the only one available at the time. To minimize lost light due to atmospheric dispersion, the position angle of the spectrograph was set to correspond to the parallactic angle for an object at airmass 1.3; below airmass ~ 1.4 the atmospheric dispersion correction is effectively negligible and most of our observations took place in this airmass range. Any lost light due to atmospheric dispersion is unlikely to significantly impact our velocity dispersion measurements as the velocity dispersion gradient of the clusters is not large. The rotation of the slit also has a negligible impact as all of these globular clusters are fairly round (Harris et al. 2002).

TABLE 1
GLOBULAR CLUSTER OBSERVATIONS AND MEASUREMENTS

ID	V [mag]	Exptime [s]	SNR	σ [km s^{-1}]
C2	18.33	10800	11	14.2 ± 2.0
C7	17.10	5400	16	22.4 ± 2.1
C11	17.70	9000	18	17.7 ± 1.9
C17	17.61	7200	19	18.9 ± 2.0
C21	17.77	10800	12	20.8 ± 1.9
C22	18.14	10800	15	19.1 ± 2.0
C23	17.19	7200	25	31.4 ± 2.6
C25	18.33	12600	5	12.2 ± 2.0
C29	17.94	14400	12	16.1 ± 2.1
C31	18.37	12600	8	15.0 ± 2.1
C32	18.31	10800	7	15.8 ± 1.4
C37	18.34	10800	10	13.5 ± 1.6
C41	18.56	19800	8	9.6 ± 2.0
C44	18.61	18000	8	9.1 ± 2.0

NOTE. — Present sample of NGC 5128 globular clusters. Cols. 1 and 2 list the cluster ID and apparent V magnitude from Peng et al. (2004a) and col. 3 our exposure times. The mean signal-to-noise ratio over the range 5000 – 6800 Å per 0.2 Å is listed in col. 4. The measured velocity dispersions and uncertainties, described in §4, are listed in column 5.

While MIKE was used to obtain both red and blue data, sufficient signal-to-noise ratio (SNR) observations of these (intrinsically red) clusters were only obtained on the red side. To enhance the SNR, the observations were binned 2×2, leading to $0.286''$ pixel^{-1} and a velocity scale of 4.2 km s^{-1}pixel^{-1}. Table 1 lists all 14 clusters according to their identification in Harris et al. (2002), along with their apparent V magnitude from Peng et al. (2004a), the total integration time, and the average SNR per pixel over the wavelength range 5000 – 6800 Å when binned to 0.2 Å pixel^{-1}. The total integration time listed is the sum of an integer number of 1800 s exposures. This exposure time was chosen to facilitate cosmic ray removal, yet also avoid a significant contribution from detector noise. Spectra of 16 velocity dispersion templates were also obtained, ranging in spectral type from G through M stars and luminosity classes from IV through I. These templates were observed in a similar manner to the globular clusters. Typically three integrations of a few seconds each were obtained for each template. Arc lamps for wavelength calibration were obtained before or after the observations of each target. Several sets of flatfield exposures using a quartz lamp were also obtained over the course of the seven-night observing run.

3. DATA PROCESSING

The data were processed with a combination of tasks from the IRAF[1] echelle package and the sky-subtraction software described by Kelson (2003). All images were overscan-subtracted and a simple cosmic-ray cleaning algorithm was applied to the individual cluster exposures. The images were also rotated such that the dispersion direction was approximately parallel to the rows of the detector. Inspection of the

[1] IRAF is distributed by the National Optical Astronomy Observatories, which are operated by the Association of Universities for Research in Astronomy, Inc., under cooperative agreement with the National Science Foundation.

several sets of flatfield exposures obtained over the course of the run showed no measurable variation and all of the flatfield exposures were therefore summed to produce one master flatfield. This flat was then normalized with low-order fits to each order and divided into all of the object exposures prior to sky subtraction.

Sky subtraction of MIKE data is complicated by the nonlinear transformation between the orthogonal (dispersion, spatial) and "natural" detector (row, column) coordinate systems and the slight undersampling of the data. The marginally undersampled sky lines are tilted with respect to the detector coordinate system and this tilt angle varies as a function of spatial position. As discussed in detail by Kelson (2003), the classical approach of rectifying and rebinning the image prior to sky subtraction can result in significant residuals in the case where the sky lines are critically- or undersampled. Superior sky subtraction can be obtained if a sky model is calculated and subtracted prior to any rectification and rebinning of the data.

The key to this technique is to calculate the transformation between the array coordinates (x,y) and the orthogonal dispersion and spatial coordinate system (x_r,y_t). By collapsing the spectrum along the spatial coordinate y_t, the profile of each sky line can then be measured as a function of the coordinate x_r in which the sky line is well-sampled (due to the tilt of the observed spectrum). A two-dimensional sky model can then be constructed with the same pixelization as the original data, thus avoiding the residuals that result from rebinning marginally or undersampled data. To employ Kelson's method, we first calculated the transformation $y_t = Y(x,y)$ with his `getrect` command, using a flatfield frame to trace the boundaries of each order. These boundaries were defined with `findslits` (treating them as individual slits in a multislit mask). We then calculated $x_r = X(x,y_t)$ with `getrect` applied to each order. Accurate calculation of this transformation requires several lines per order. As there are few airglow lines in the higher orders (shorter wavelengths), we created a composite image of spectroscopic lines by combining a very high SNR sky frame (calculated by summing a large number of our exposures of the fainter clusters) with ThAr and NeAr lamp spectra. As many ThAr lines saturated in the 13 reddest orders, these orders were masked out before construction of the composite line image for `getrect`. A sky model image for each globular cluster exposure was then calculated with `skyrect` and subtracted from the flatfielded data. Observations of the template stars were sufficiently short that no sky subtraction was deemed necessary.

The dispersion solution was calculated with the `ecidentify` task in the IRAF echelle package and ThAr lamp spectra. Although most of the reddest orders were saturated by bright lines as described above, a combination of multiple lines in the bluer orders and several unsaturated lines in the redder orders led to a good solution (rms $\sim$ 0.005 – 0.007 Å) with a fourth-order Legendre polynomial in x and y. All of the object spectra were then extracted with `apall`. Because most of the individual cluster spectra were too faint for a good trace, particularly in the bluest orders, we used a reference trace from a brighter object. This trace was recentered based on the centroid of the cluster trace in the reddest, highest SNR orders. Each individual exposure was extracted in this manner as several-pixel shifts were observed between a small number of the multiple exposures on individual clusters. The width of the spectral extraction window was 9 pixels or 2.6″. The arc lamp was extracted for each object with the same trace and the dispersion solution was calculated with the `ecreidentify` task. The spectra were then placed on a linear wavelength scale with the `dispcor` task for measurement of their line-of-sight velocity dispersion σ. Template stars and the flux standard HR 1544 were extracted in a similar manner. Orders 68 – 39 of C23, the cluster with the highest SNR, are shown in Figure 1. The calcium triplet region (order 40) is shown for all 14 clusters in Figure 2. No correction for telluric absorption was applied to these data.

4. VELOCITY DISPERSION MEASUREMENT

The two most commonly employed techniques for velocity dispersion measurement are direct-fitting in pixel space (e.g. Rix & White 1992; Kelson et al. 2000; Barth et al. 2002) and cross-correlation techniques in the Fourier domain (e.g. Illingworth 1976). After experiments with both techniques we chose the cross-correlation method developed in detail by Tonry & Davis (1979) as implemented by the `rvsao` package (Kurtz & Mink 1998) in IRAF. The main advantage of the cross-correlation function (hereafter CCF) is that it is less sensitive to the relative line strengths in the targets and templates. This is likely to be the case for the present study due to metallicity differences between the globular clusters and the Galactic template stars observed. Trial implementations of direct-fitting in pixel space confirmed that most of the stellar templates are not good matches in detail to these globular clusters. Direct pixel-fitting did show that the observed stellar templates with spectral types between G8 and K3 were the best matches to the globular cluster spectral energy distributions. The stellar templates used for this study are: HD 80499 (G8III), HD 95272 (K0III), HD 88284 (K0III), HD 43827 (K1III), HD 92588 (K1IV), HD 44951 (K3III), and HD 46184 (K3III).

The first step in implementation of the CCF technique is the calculation of the relation between the CCF width and the observed line-of-sight velocity dispersion σ. To measure this relationship, we convolved a range of the observed stellar templates by Gaussian functions with σ = [5,7,10,14,20,28,40,56] km s^{-1}and used a simple spline fit to calculate the relation between CCF width and input σ. We calculated this relationship for each of the spectroscopic orders and determined that the uncertainty in σ measurements in orders with significant telluric absorption (50, 48, 47, 45, 42, and 41) was considerably higher than those without. Given the large number of orders available, these orders were excluded from subsequent analysis. Based on measurements from the remaining orders we determined that all of the globular clusters have σ in the approximate range of 10 – 30 km s^{-1}. The velocity dispersions of these clusters are thus well-resolved by this instrument configuration.

While the CCF technique is known to be relatively insensitive to template mismatch, we tested the importance of this potential source of systematic error by convolving each spectral type by the range of velocity dispersions given above and using other templates of similar but not identical temperature to measure σ (e.g. a K0III template to measure an artificially broadened K3III template). This analysis showed that template mismatch produced at most an rms uncertainty of 1 km s^{-1} when σ was calculated for a single order. Given the large number of orders available and our estimate of the range in σ of these clusters, we then experimented with combining multiple orders together as well as binning the data to improve

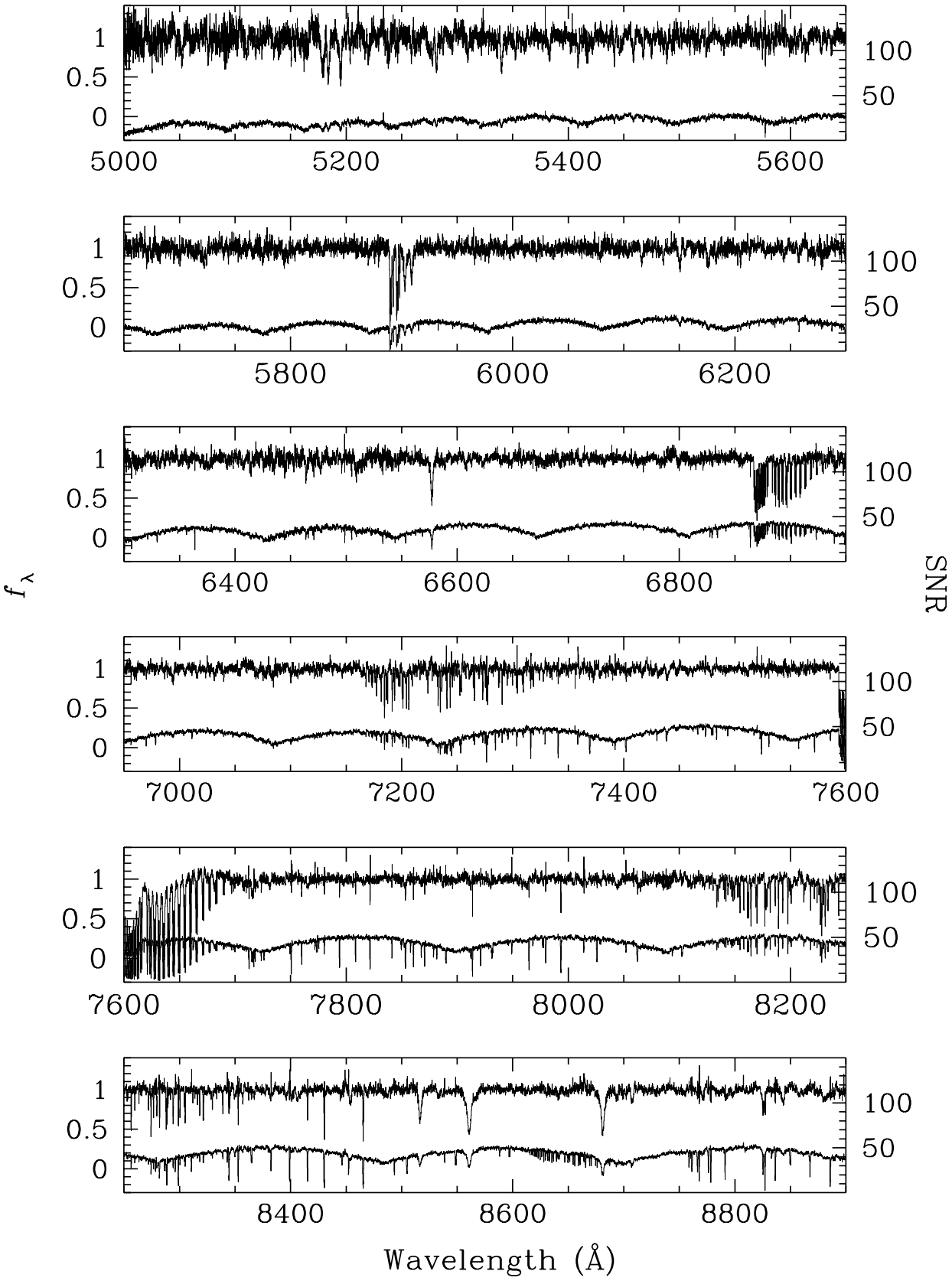

FIG. 1.—Orders 39 – 68 of the NGC 5128 globular cluster C23. Each order has been divided by a low-order polynomial fit to normalize the spectrum (*dark solid line, left axis*). The SNR as a function of wavelength is shown below the spectrum (*light solid line, right axis*). The smooth SNR variation is due to the transmission of the individual orders, which have been stiched together.

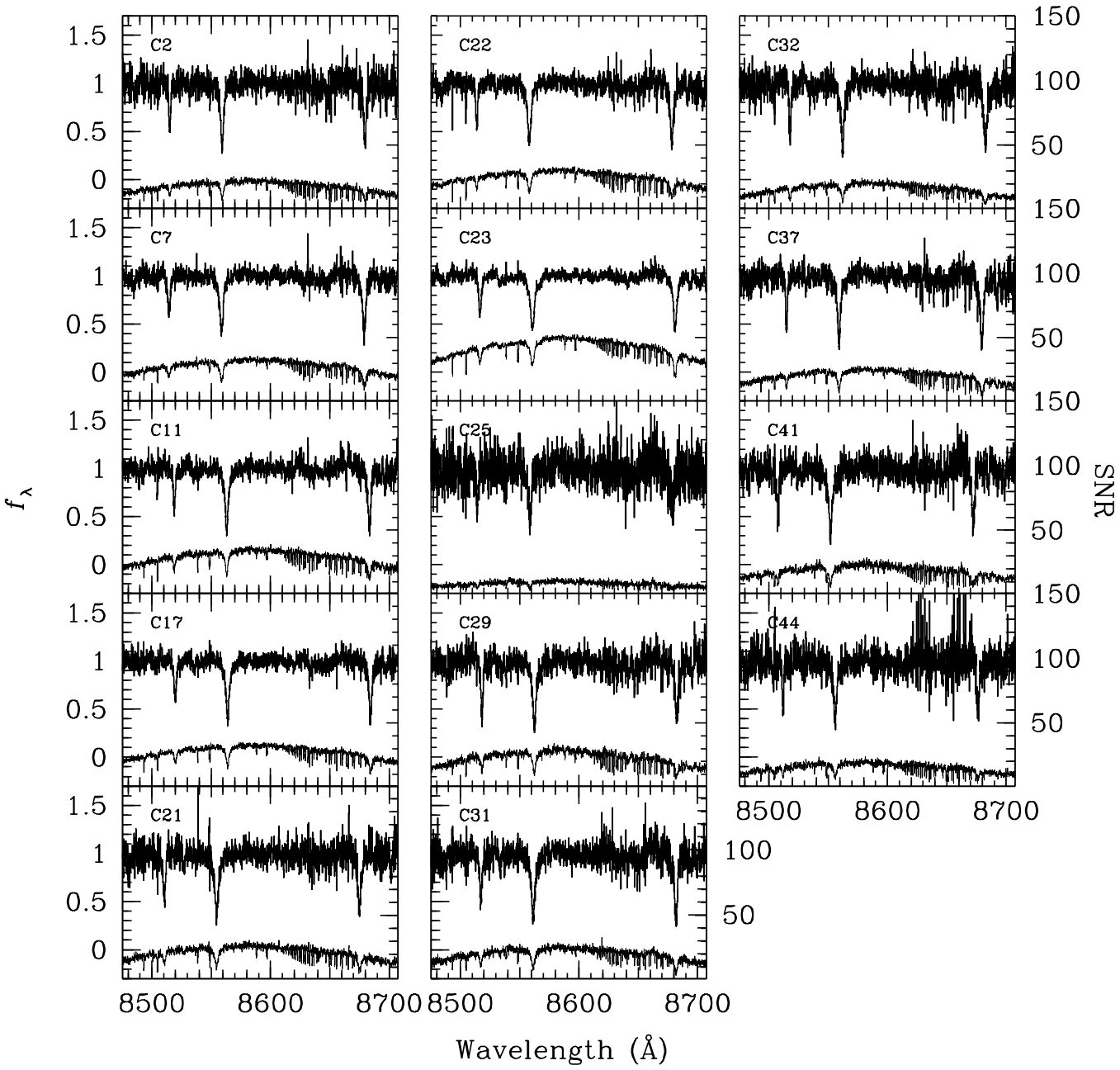

FIG. 2.—Calcium triplet region (order 40) for all 14 NGC 5128 globular clusters.

SNR. A range of tests showed we obtain excellent and very stable results over the wavelength range 5000 – 6800 Å and the spectra rebinned to a scale of 0.2 Å pixel^{-1}. The rms variation due to template mismatch over this range was less than 0.5 km s^{-1}. CCFs for all 14 clusters are shown in Figure 3 and the measured σ and estimated uncertainties are listed in Table 1.

The 5000 – 6800 Å spectral range does not include the higher SNR CaT region. While the CaT lines are quite strong for all of the clusters (see Figure 2), these lines are in fact so strong that they exhibit significant damping wings. These damping wings broaden the line profiles of the template stars significantly and they are not a good representation of the instrumental line profile. The CaT lines in the template stars have intrinsic widths comparable to or larger than the measured velocity dispersions of the globular clusters over the 5000 – 6800 Å region. We therefore did not use these lines to measure the cluster velocity dispersions. The neighboring, red orders have comparable SNR to the CaT region, although these orders are contaminated by significant telluric absorption. Although the telluric absorption is to some extent cor-

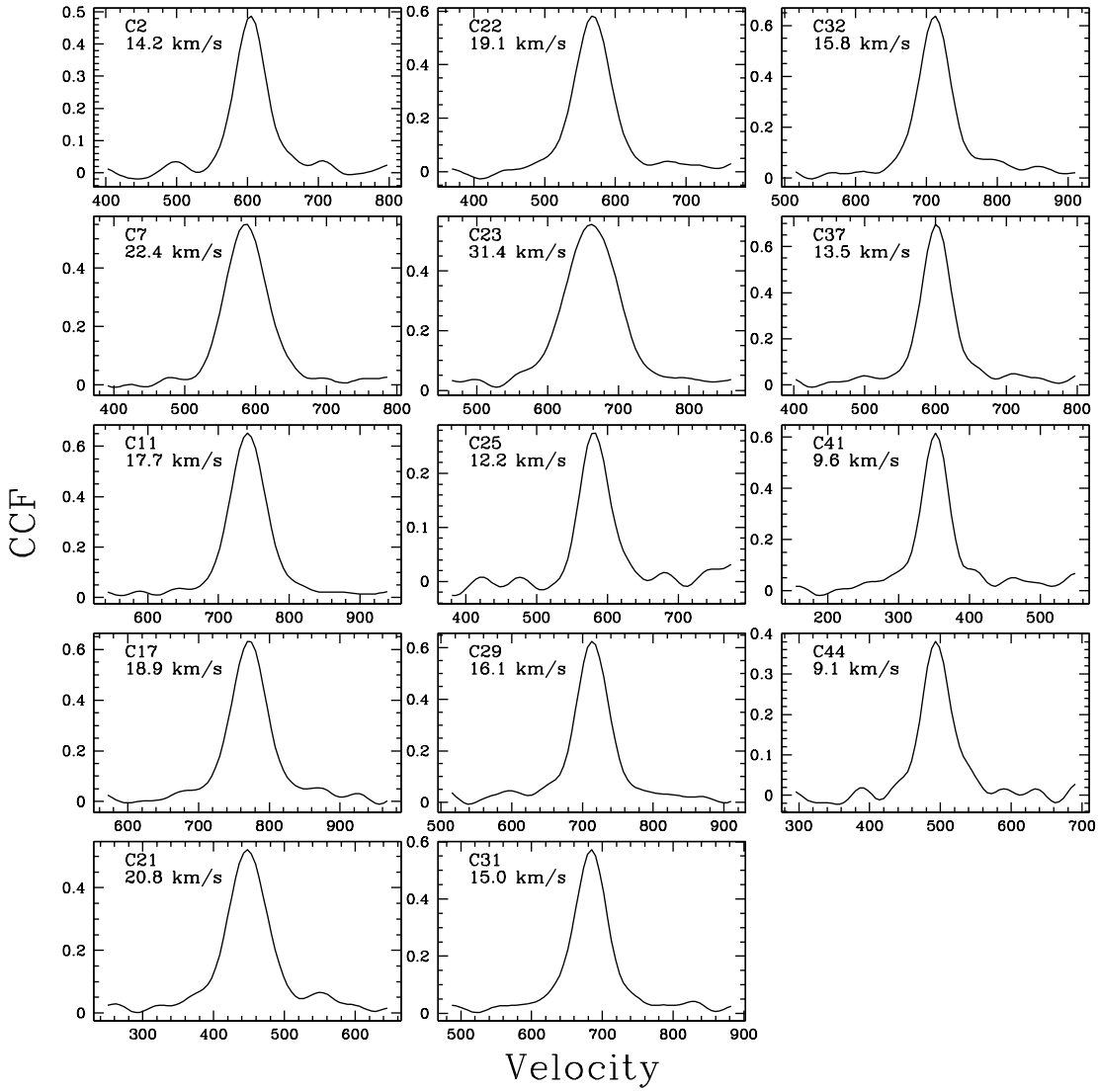

FIG. 3.—Cross-correlation function for each globular cluster over the wavelength range 5000 – 6800 Å and binned to 0.2 Å pix $^{-1}$. The derived velocity dispersion is listed in the top left corner of each panel.

rectable, these orders were also discarded for the velocity dispersion measurement because the SNR in the 5000 — 6800 Å region is sufficiently high that SNR is at most a modest contributor to the total error budget (see below). While there are still reasonably strong lines in the 5000 – 6800 Å region, notably Mg*b* and Hα, these lines only make a minor contribution to the velocity dispersion measurement.

Given the range of SNR and σ of these data, we performed simulations with our template stars to determine the quality of our measurements as a function of both SNR and σ. These tests were performed by first convolving the best-fitting template (HD 88284) with the range of velocity dispersions described above. We then added noise to these convolved spectra to produce a set of output spectra with average SNR of [2,4,8,16,32,64,128] for each velocity dispersion. As the SNR per pixel is quite variable due to both the blaze function and the red color of these clusters, we used an input SNR spectrum from one of the cluster observations (C23, shown in Figure 1) to reproduce the pixel-to-pixel variation in the SNR, while forcing the mean SNR in the spectra to equal the specified values. The widths of these input spectra were then calculated in a similar fashion to the globular cluster measurements described above. The results of this analysis for $\sigma = 10-28$ km s^{-1}(the range most appropriate to this study) are shown in Figure 4. This figure displays the difference between the input σ and the measured σ at a given SNR, normalized by the input σ.

As expected, the deviation between the input σ and the measured σ increases toward lower SNR. In particular, these simulations show that at lower SNR the measurements will tend to overestimate σ. This may be because the addition of noise systematically erases narrower features more readily than broader features. The simulations also show that at a given SNR the velocity dispersion measurement will be more accurate if the intrinsic velocity dispersion is lower. This is likely a reflection of the net SNR over the number of pixels

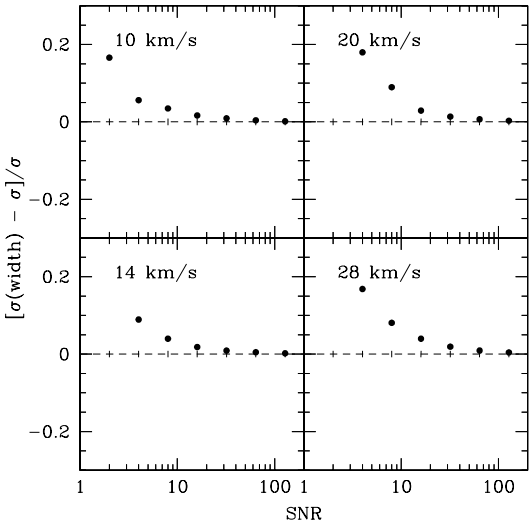

FIG. 4.—Velocity dispersion residuals as a function of signal-to-noise ratio for the spectral region 5000 – 6800 Å and binned to 0.2 Å pix^{-1}. The σ values shown closely correspond to the observed range for the NGC 5128 globular clusters. Less than half of the cluster observations have mean SNRs below ten. Tickmarks along the dashed line mark the location of the model SNR values. Only the panel for σ = 10 km s^{-1}plots a residual value for SNR= 2. The residuals were larger than 30% at SNR= 2 for the remaining three velocity dispersions.

that comprise a given feature. The fewer pixels that span, e.g. the absorption lines employed here, the higher the net SNR of the feature relative to a spectrum of the same mean SNR per pixel with a larger σ. This systematic effect on the σ measurement impacts our observations at most at the 5% level. Three of the clusters with velocity dispersions of on order 10 km s^{-1}(C25, C41, C44) have a mean SNR less than 10 over then 5000 – 6800 Å range in our rebinned spectra, while three (C2, C31, C32) in the 14 km s^{-1}range have a mean SNR $\sim$ 10 (see Table 1). The measured velocity dispersions for these low-SNR clusters have been adjusted to account for the expected overestimate. The remaining clusters do not suffer from systematic errors due to low SNR.

The resolution of our rebinned spectra could also impact the measured σ as the velocity dispersion resolution now varies from 12 km s^{-1}at 5000 Å to 8.8 km s^{-1}at 6800 Å. However, measurements of σ with a dispersion of 0.1 Å pixel^{-1} yield consistent results with the values in Table 1, although with somewhat larger scatter due to the lower SNR. The relationship between measured σ and SNR at each σ shown in Figure 4 also demonstrates that the measured σ converges to the input value as the SNR increases. The measured values quoted in Table 1 also agree well with measurements obtained from single, unbinned orders and direct-pixel fitting, although the latter approaches have larger scatter. We note that preliminary velocity dispersions measurements from high-resolution spectroscopy of four NGC 5128 globular clusters were obtained by Dubath and reported in Harris et al. (2002). These measurements are marginally consistent with our own.

The $1'' \times 2.6''$ spectral extraction window we employed corresponds to a physical area of 18.6×48.4 pc, which is larger than the half-light radius for all of these clusters (e.g. see Table 2). In King models for globular clusters, the velocity dispersion is a function of radius. Our measurements, because they include most of the cluster, should correspond well to the global, one-dimensional velocity dispersion σ_∞. In contrast, the core one-dimensional velocity dispersion σ_0 is approximately the quantity measured for Galactic globular clusters and the most commonly quoted quantity in the literature. The core value σ_0 is larger than σ_∞ in the King models and the degree of difference depends on cluster concentration. For the clusters studied here, this correction is on order 5 – 10% for the range of cluster concentrations in this sample (see e.g. Djorgovski et al. 1997). The errorbars quoted in Table 1 include the uncertainties in this correction, which are caused by uncertainties in the measured structural parameters reported by Harris et al. (2002) and the exact placement of the slit, as well as the uncertainties due to template mismatch and SNR.

5. ANALYSIS

5.1. *Observed Cluster Properties*

These 14 globular clusters are the brightest clusters with King model structural parameters measured with *HST* by Harris et al. (2002). These models are described by the parameters W_0 (central potential), r_c (core radius) and c (cluster concentration, where $c = \log r_t/r_c$ and r_t is the tidal radius). Harris et al. (2002) also fit for ellipticity. Both r_c and r_h (the model half-mass radius) from their fits are provided in Table 2, converted to parsecs, and their measurement of c is also given. The projected half-light radius is $R_h \approx 0.73 r_h$. As these values span the approximate range of $1.4 < c < 2.1$, none are core-collapse clusters. All 14 of these clusters were also included in the recent study by Peng et al. (2004a), who have obtained *UBVRI* photometry and radial velocities for over 200 NGC 5128 globular clusters. As most of the Harris et al. (2002) photometry is from unfiltered STIS images, we have listed instead the Peng et al. (2004a) V_0, $(B-V)_0$, and $(V-I)_0$ values in the table, where these quantities have been dereddened based on their quoted $E(B-V)$ and assuming R_V = 3.1. We also include the central surface brightness μ_V^0 from Harris et al. (2002), but recalibrated by the difference between their quoted V magnitudes and those in Peng et al. (2004a), and have calculated the mean, reddening-corrected surface brightness within the projected half-light radius: $\langle \mu_V \rangle_h = V_0 + 0.75 - 2.5 \log \pi R_h^2$. All of these dereddened values only account for Galactic dust and do not include any dust intrinsic to NGC 5128. While most of these clusters are not near NGC 5128's prominent dust lane, dust may affect the colors of some of these clusters.

The color distribution of NGC 5128 globular clusters is bimodal (Held et al. 1997; Peng et al. 2004a), similar to the globular cluster systems of many galaxies (e.g. Larsen et al. 2001; Kundu & Whitmore 2001). A bimodal color distribution is most commonly ascribed to a bimodal distribution in metallicity as color is a reasonable proxy for metallicity in old single stellar populations. In the case of NGC 5128, this galaxy appears to have undergone a major merger in the recent past. Based on the strength of Hβ, Peng et al. (2004a) conclude that the more metal-rich globular clusters formed 5^{+3}_{-2} Gyr ago, while Kaviraj et al. (2004) derive an age estimate of 1 – 2 Gyr for the metal-rich population in their study of the metallicity distribution function (derived from the Peng et al. (2004a) U and B photometry). Figure 5 shows the $(B-V)_0$ and $(V-I)_0$ color distributions for all of the globular clusters

TABLE 2
STRUCTURAL AND PHOTOMETRIC MEASUREMENTS

ID	r_c [pc]	r_h [pc]	c	μ_V^0	$\langle\mu_V\rangle_h$	V_0	M_V	$(B-V)_0$	$(V-I)_0$
C2	0.80	8.49	1.99	16.27	17.70	18.10	-9.82	0.70	0.86
C7^x	1.41	10.00	1.83	15.46	16.79	16.83	-11.09	0.75	0.91
C11	1.30	10.41	1.88	16.19	17.58	17.54	-10.38	0.93	1.11
C17	2.27	7.60	1.43	16.14	16.65	17.29	-10.63	0.77	0.88
C21	1.21	9.27	1.86	15.97	17.32	17.53	-10.39	0.78	0.93
C22	1.10	5.06	1.62	15.60	16.29	17.81	-10.11	0.79	0.91
C23^x	0.87	4.41	1.67	14.37	15.06	16.88	-11.04	0.96	1.10
C25^x	0.99	8.32	1.90	16.34	17.71	18.15	-9.77	0.96	1.14
C29^x	1.19	9.16	1.87	16.21	17.52	17.75	-10.17	0.87	1.05
C31	0.91	5.29	1.74	15.71	16.58	18.01	-9.91	0.92	1.12
C32^x	0.56	7.24	2.06	15.88	17.33	18.07	-9.85	0.94	1.10
C37^x	0.58	4.43	1.87	15.31	16.28	18.09	-9.83	0.84	0.99
C41	0.78	5.99	1.87	15.94	17.04	18.19	-9.73	0.87	1.06
C44	1.25	7.60	1.70	16.45	17.68	18.32	-9.60	0.68	0.84

NOTE. — Structural and photometric parameters of our sample based on measurements from the literature. For each cluster in column 1 we list r_c, r_h, c, and μ_V^0 from Harris et al. (2002) in cols. 2–5, where we have adopted a distance to NGC 5128 of 3.84 Mpc. Col. 6 contains the mean surface brightness within the projected half-light radius, while cols 7–10 are the reddening-corrected V_0 magnitude, the absolute V magnitude, and the $(B-V)_0$ and $(V-I)_0$ colors from Peng et al. (2004a). We have used this photometry to apply a correction to μ_V^0 (see text) and calculate $\langle\mu_V\rangle_h$. The six clusters marked with an x superscript indicate that Harris et al. (2002) found evidence for extratidal light in their surface photometry.

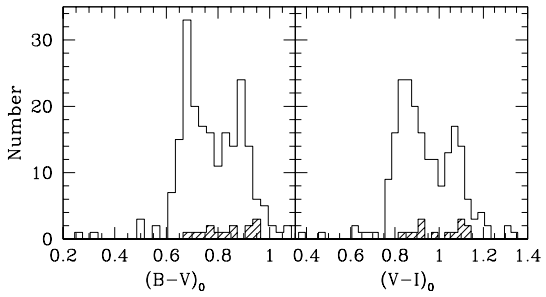

FIG. 5.—Reddening-corrected colors of NGC 5128 globular clusters. All clusters observed by Peng et al. (2004a) are shown in the histogram, while the globular clusters in the present study are in the hatched histogram. The latter clusters span a range in color representative of the NGC 5128 globular cluster system.

studied by Peng et al. (2004a). The clusters in the present study are represented by the hatched histogram and span the full range in color of the majority of the NGC 5128 globular cluster system. Figure 6 demonstrates that these clusters do not show any strong correlations between color and velocity dispersion, central concentration, mass, or mass-to-light ratio (see next section).

5.2. *Cluster Masses and Mass-to-Light Ratios*

One of the most valuable and readily calculated properties of a globular cluster is its total mass. There are multiple ways to estimate the mass of a globular cluster, although the most straightforward approach is to use the virial theorem:

$$M_{vir} = 2.5\,\frac{\langle v^2\rangle\, r_h}{G}, \qquad (1)$$

where $\langle v^2\rangle \approx 3\sigma^2$ is the mean-square speed of the cluster stars and r_h is the half-mass radius (Binney & Tremaine 1987). The virial masses for these clusters (in units of 10^6 $M_\odot$) are listed in Table 3.

TABLE 3
MASSES AND MASS-TO-LIGHT RATIOS

ID	M_{vir} [$M_{\odot,6}$]	M_{King} [$M_{\odot,6}$]	μ_{King}	$\Upsilon_{V,\odot}$	log E_b [erg]
C2	2.99 ± 0.67	1.74	52.4	4.1 ± 1.6	52.16
C7^x	8.75 ± 1.46	5.85	39.7	3.7 ± 0.9	53.10
C11	5.69 ± 1.04	3.64	43.0	4.7 ± 1.3	52.68
C17	4.73 ± 0.86	3.84	21.7	3.1 ± 0.7	52.82
C21	7.00 ± 1.15	4.52	41.7	5.7 ± 1.5	52.92
C22	3.22 ± 0.59	2.43	28.6	3.4 ± 0.8	52.61
C23^x	7.59 ± 1.21	5.61	30.9	3.4 ± 0.7	53.40
C25^x	2.16 ± 0.52	1.35	44.5	3.1 ± 1.2	51.93
C29^x	4.14 ± 0.87	2.71	42.3	4.1 ± 1.3	52.47
C31	2.07 ± 0.47	1.48	34.4	2.6 ± 0.8	52.16
C32^x	3.15 ± 0.51	1.74	60.8	4.2 ± 1.2	52.24
C37^x	1.41 ± 0.28	0.92	42.3	1.9 ± 0.6	51.85
C41	0.96 ± 0.30	0.63	42.3	1.4 ± 0.7	51.39
C44	1.10 ± 0.36	0.70	32.3	1.8 ± 0.9	51.41

NOTE. — Derived parameters for NGC 5128 globular clusters. For each cluster in column 1, the virial mass and King model masses (in units of 10^6 $M_\odot$) are listed in columns 2 and 3. The dimensionless King mass, mass-to-light ratio, and binding energy are provided in columns 4 – 6.

An alternative approach is to use the King parameters to calculate the cluster mass. From Illingworth (1976), the mass is

$$M_{King} = 167\, r_c\, \mu\, \sigma_0^2, \qquad (2)$$

where μ is the dimensionless King model mass (King 1966) and σ_0 is the core velocity dispersion (see also Richstone & Tremaine 1986). As discussed previously, we have estimated σ_0 from the cluster concentration parameter (Djorgovski et al. 1997). The dimensionless mass μ is also a function of concentration. The King model masses for these clusters are $\sim 50\%$ less than the virial mass estimates. It is not unusual for these two estimates to disagree (e.g. see Meylan et al. 2001, for

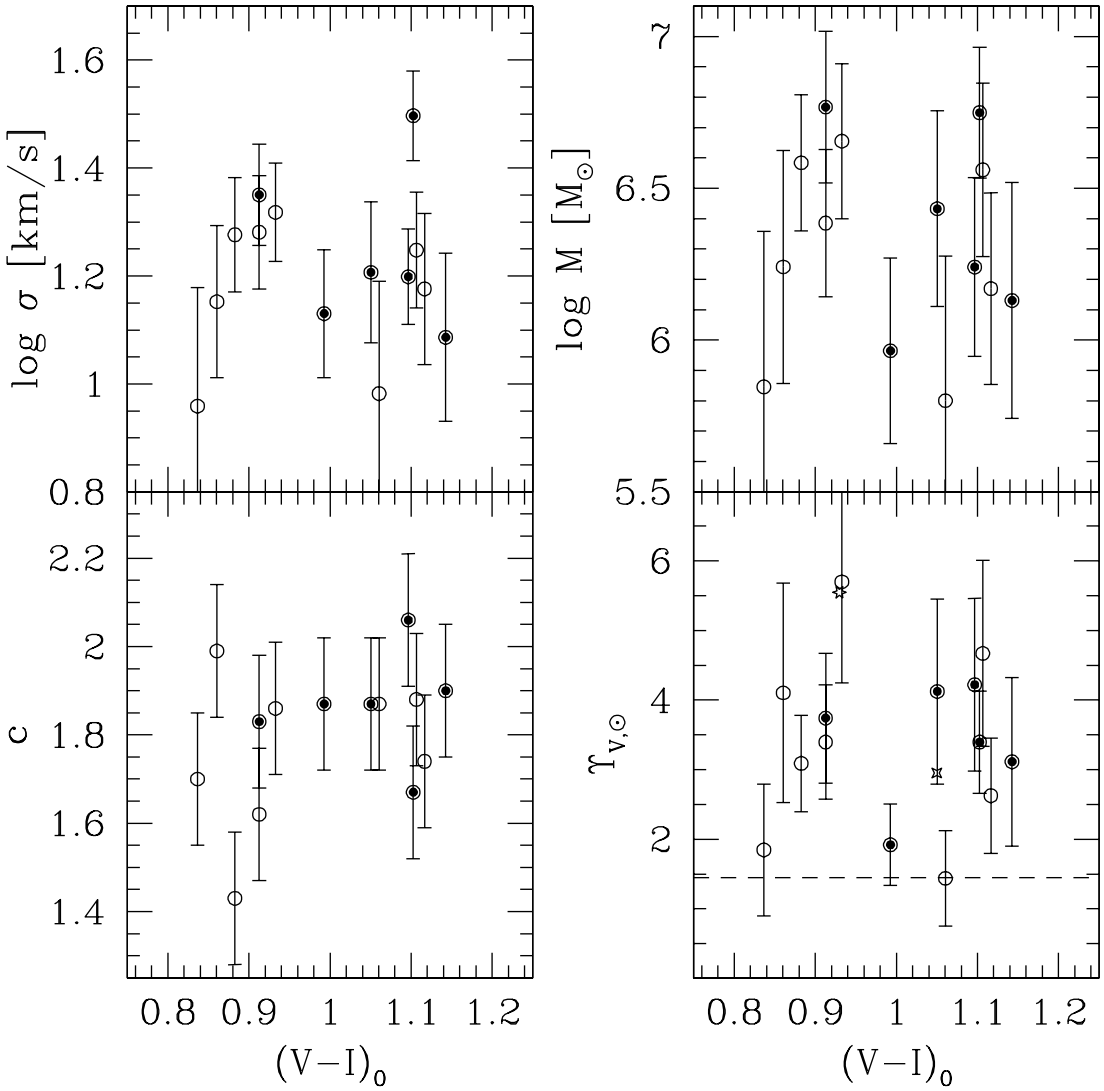

FIG. 6.—Reddening-corrected $V-I$ color of NGC 5128 globular clusters as a function of velocity dispersion (*upper left*), central concentration (*lower left*), virial mass (*upper right*), and mass-to-light ratio (*lower right*). All NGC 5128 clusters are marked with circles, while clusters identified by Harris et al. (2002) to possibly have extratidal light are marked with partly filled circles. The dashed line in the lower-left panel represents the mean core mass-to-light ratio derived by McLaughlin (2000) for Galactic globular clusters. The 0.18 magnitude uncertainty in the NGC 5128 distance modulus (Rejkuba 2004) translates into an additional, systematic uncertainty of $\sim 18\%$ in the mass-to-light ratio. ωCen (*cross*) and G1 (*star*) are also shown in this panel.

ωCen and G1). The uncertainties (not shown) in the King masses are larger than the virial mass estimates due to uncertainties in the measurement of c and r_c, in addition to the uncertainties in σ. We therefore use the virial mass in the subsequent discussion.

Once the mass has been estimated, the V–band mass-to-light ratio in solar units $\Upsilon_{V,\odot}$ is readily calculated. The virial mass is divided by the V–band luminosity $L_{V,\odot}$, which is computed from the reddening-corrected magnitude V_0 (assuming $M_{V,\odot} = 4.83$). The mass-to-light ratios for these clusters are listed in column 5 of Table 3. These values fall in the range 1.4 – 5.7 and have an average value of $\langle\Upsilon_{V,\odot}\rangle \sim 3$. This average is larger than the mean core mass-to-light ratio of 1.45 ± 0.1 for globular clusters in the Galaxy (McLaughlin 2000) and the comparable core and global values of 1.53 ± 0.18 from four globular clusters in M33 (Larsen et al. 2002). If we had adopted the King mass estimates to compute the mass-to-light ratios, rather than the virial mass estimates, the mass-to-light ratios would be $\sim 50\%$ less. The difference between the NGC 5128 globular clusters and those in the Local Group may be due to either intrinsic differences or due to measurement uncertainties. If the latter is the case, then the masses are overestimated, the luminosities are underestimated, or both. An overestimate in the mass could be explained by either an overestimate of σ by $\sim 50\%$ or an overestimate of r_h by a factor of 2, although both of these possibilities vastly exceed the estimated uncertainties in these quantities. The mass-to-light ratios between the different globular cluster systems could also be brought into agreement if the luminosities are underestimated by a factor of 2. This exceeds the estimated uncertainty

in the distance to NGC 5128 (Rejkuba 2004), although intrinsic reddening could also contribute and NGC 5128 is well-known for its prominent, large dust lanes. The luminosities could also be underestimated if there is a significant contribution to the surface brightness at large radii, where the SNR is poor. While a conspiracy of all of these potential sources of error could bring the mean mass-to-light ratios of these globular cluster systems into agreement, we conclude that the differences are likely real.

Further support of these large mass-to-light ratios is provided by some of the most massive globular clusters in the Local Group, including the Galactic globular cluster ωCen, which has $\Upsilon_{V,\odot} = 2.4-3.5$ and G1 in M31 with $\Upsilon = 3.6-7.5$ (Meylan et al. 1995, 2001). The lower-right panel of Figure 6 shows the mass-to-light ratios for the NGC 5128 globular clusters as a function of $(V-I)_0$. No obvious trend with color is apparent, as might be expected if the generally redder, more metal-rich clusters identified by Peng, Ford, & Freeman (2004b) formed more recently. The massive, Local Group clusters ωCen and G1 are also shown for comparison. For these clusters the average of the virial and King mass estimates from Meylan et al. (2001) were used for the mass-to-light ratio, while the integrated colors are either from the Harris (1996) compilation (ωCen) or from Heasley et al. (1988).

5.3. *Fundamental Plane*

NGC 5128 has a significantly larger population of the most massive and luminous globular clusters than any galaxy in the Local Group. Our cluster sample is dominated by these clusters due to observational constraints, yet this population is arguably the most interesting as they provide an opportunity to verify and extend relationships for local clusters to more extreme examples of the population. The clusters in our sample are comparable in mass to ωCen, the most massive Galactic globular cluster at $M = 5\times10^6$ M$_\odot$(Meylan et al. 1995) and M31's G1, which with $M = (7-17)\times10^6$ M$_\odot$(Meylan et al. 2001) is the most massive cluster known in the Local Group.

The main relationship of interest is the globular cluster fundamental plane, the approximately two-dimensional structure occupied by clusters in the three-dimensional space defined by, e.g. central velocity dispersion, surface brightness, and core radius. Djorgovski (1995) demonstrated that the plane occupied by globular clusters is consistent with the expectations for virialized cluster cores,

$$r_c \sim \sigma_0^2 I_0^{-1} \Upsilon^{-1}, \tag{3}$$

and a constant mass-to-light ratio. This appears to be the case for both the core properties as well as properties derived at the half-light radius, with the differences between these two regimes due to the degree of central concentration.

In the top panels of Figure 7 we plot two projections of the core fundamental plane from Djorgovski (1995) for the NGC 5128 globular clusters, along with clusters in the Milky Way, M31, M33, and the Magellanic Clouds. These projections show that the NGC 5128 clusters are relatively large and have higher surface brightnesses than Galactic clusters, although are more similar to globular clusters studied in other Local Group galaxies. Half-light projections (*bottom panels*) show all of these globular cluster systems follow similar trends to the Milky Way system, although extragalactic globular clusters appear to have systematically lower mean surface brightness within the half-light radius for a given σ. This may reflect a bias toward selection of bright objects that nevertheless appear marginally resolved in ground-based images or a relative overestimate of R_h for more distant clusters.

Numerous literature sources were employed to obtain data for globular clusters in the Local Group. Data for the Milky Way were obtained from Pryor & Meylan (1993) and Harris (1996). Velocity dispersion data for M31 were obtained from Dubath & Grillmair (1997) and Djorgovski et al. (1997), while structural parameters were obtained from Barmby et al. (2002) or earlier work (Battistini et al. 1982; Crampton et al. 1985; Bendinelli et al. 1993; Fusi Pecci et al. 1994; Rich et al. 1996; Grillmair et al. 1996). Data for the Magellanic Clouds were obtained from Dubath et al. (1997) and data for M33 were obtained from Larsen et al. (2002), while the photometry for the latter was dereddened with the $E(V-I)$ values derived by Sarajedini et al. (1998). Data for the three Fornax dwarf galaxy's globular clusters with velocity dispersion measurements and structural parameters were obtained from Dubath, Meylan, & Mayor (1992) and Mackey & Gilmore (2003).

McLaughlin (2000) has recently recast discussion of the fundamental plane for globular clusters in terms of mass-to-light ratio, luminosity, binding energy, and Galactocentric radius. In the context of the four independent parameters that characterize single-mass, isotropic King models, he found that Galactic globular clusters could be described with a constant mass-to-light ratio and a binding energy regulated only by luminosity and Galactocentric radius: $E_b = 7.2\times10^{39}(L/L_\odot)^{2.05}(r_{gc}/8\,\mathrm{kpc})^{-0.4}$ erg. Figure 8 shows that NGC 5128 clusters follow approximately the same relation between binding energy and luminosity as Milky Way and other globular clusters in the Local Group, although the NGC 5128 and other clusters with higher estimated M/L fall above the relation traced by Milky Way clusters. We did not explore a dependence of binding energy on projected galactocentric radius due to distance uncertainties.

6. CONNECTION TO OTHER SPHEROIDAL SYSTEMS

Many efforts over the years have investigated the connection between globular clusters and other spheroidal systems. One valuable approach is the κ–space formalism developed by Bender et al. (1992). This space is comprised of three orthogonal axes that are proportional to mass (κ_1), mass-to-light ratio (κ_2), and a third perpendicular axis that scales as surface brightness cubed times mass-to-light ratio (κ_3). Burstein et al. (1997) compiled κ–space coordinates for a large number of spheroidal systems, with masses from globular cluster scales to clusters of galaxies. For globular clusters, the κ–space coordinates are derived as

$$\kappa_1 = (\log\sigma_e^2 + \log r_e)/\sqrt{2} + 0.11 \tag{4}$$

$$\kappa_2 = (\log\sigma_e^2 + 2\log I_e - \log r_e)/\sqrt{6} + 0.06 \tag{5}$$

and

$$\kappa_3 = (\log\sigma_e^2 - \log I_e - \log r_e)/\sqrt{3} + 0.09, \tag{6}$$

where $\sigma_e \approx \sigma_\infty$, $r_e \approx r_h$, and I_e is the mean surface brightness within r_e in units of B–band solar luminosities per square parsec.

In Figure 9 we plot the three κ–space projections of the fundamental plane for NGC 5128 clusters (*open circles*), along with Galactic globular clusters (*crosses*), those in M31 (*stars*), and galaxies (*diamonds* and *open triangles*, data from Burstein et al. 1997). This figure indicates that the NGC 5128 clusters are quite similar, although systematically more massive, than the Galactic clusters. In the κ_1 coordinate, globular clusters are clearly separated from galaxies. This does not necessarily rule out the existence of objects in this gap, as a simple extrapolation of the mass functions for both globular

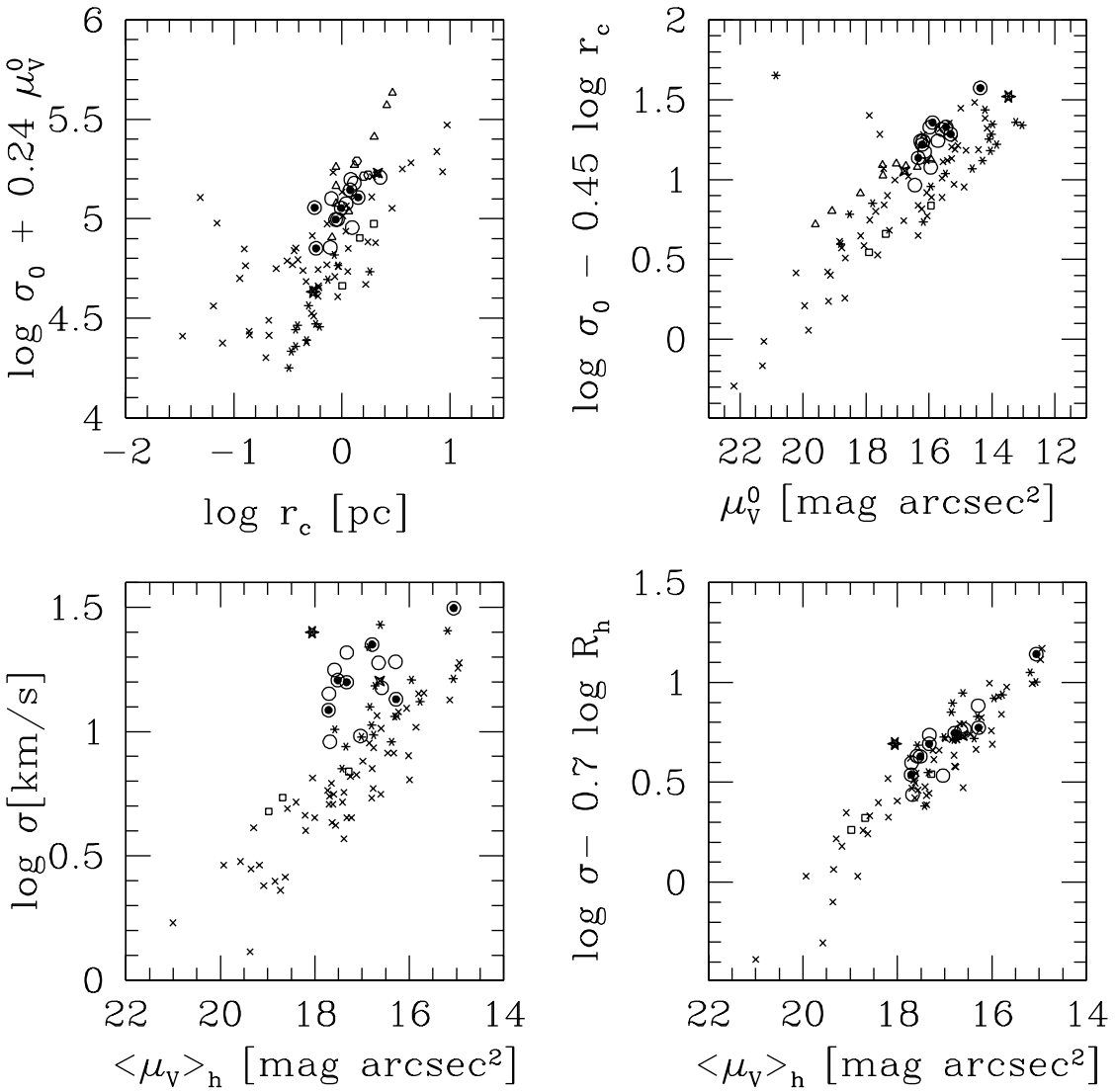

FIG. 7.—Core and half-light fundamental plane correlations for globular clusters. The core fundamental plane projections (*top panels*) demonstrate that the NGC 5128 clusters (*open circles*), including those with possible extratidal light (*partly filled circles*), approximately follow the same relations as globular clusters in the Local Group. These globular cluster systems include those for our Galaxy (*crosses*), M31 (*stars*), M33 (*squares*), the Magellanic Clouds (*triangles*), and the Fornax dwarf galaxy (*pentagons*). Half-light parameters (*bottom panels*) show comparable relations. Data were culled from the literature sources cited in the text.

cluster systems and dwarf galaxies suggest that such objects should be extremely rare and, in the case of dwarf galaxies, quite difficult to detect. Simple scaling arguments suggest that globular cluster systems in massive ellipticals such as NGC 5128 are arguably the best place to identify objects in this region, provided there is not some other physical mechanism that sets a maximum globular cluster mass. The globular clusters in the present study are a step toward eliminating the mass gap.

There is also a separation in the κ_3 coordinate (M/L) between globular clusters and galaxies, although not as stark as κ_1 (see Figure 9, *left panel*). The mean mass-to-light ratio of Galactic globulars is 1.45 (McLaughlin 2000), and Larsen et al. (2002) found a comparable number for M33. While the higher mass-to-light ratio for NGC 5128 clusters is somewhat surprising, this may be a common feature of more massive clusters. For example, the mass-to-light ratios of ωCen and G1 are in the same range as those in NGC 5128, as are the mass-to-light ratios (or κ_3 values) of other massive clusters in the Galaxy and M31. The κ_3 values for dwarf and regular elliptical galaxies are higher than for most globular clusters, reflecting their larger mass-to-light ratios, although they overlap with the most massive globular clusters. The fundamental plane relationship for spheroidal galaxies requires $\Upsilon_V \propto L_V^{0.2}$ (van der Marel 1991; Magorrian et al. 1998). A relationship between mass (or luminosity) and mass-to-light ratio for the most massive globular clusters is suggested by their apparently higher κ_3 values.

The κ_2 ($I_e^3 \times M/L$) coordinate is essentially an indicator of surface brightness at the effective radius as its dependence on M/L is much weaker than I_e. κ_2 exhibits a great deal of overlap in the properties of all spheroidal systems. In fact, the

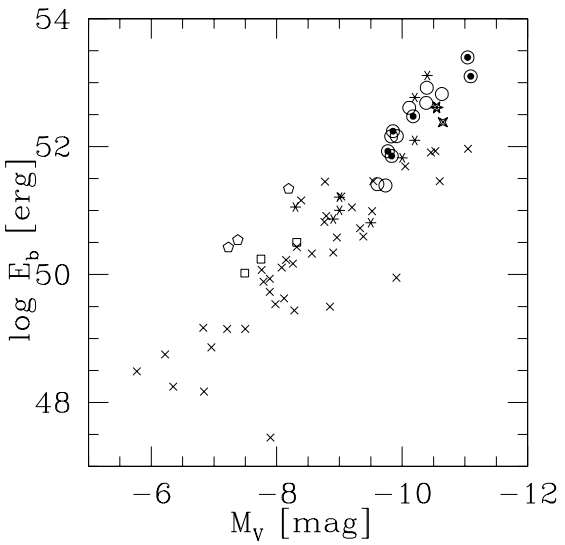

FIG. 8.—Binding energy vs. absolute *V* magnitude for globular clusters. The NGC 5128 globular clusters (*circles*) follow approximately the same relation found by McLaughlin (2000) for Galactic clusters (*crosses*), although they diverge somewhat toward higher binding energy for a given M_V. Clusters from M31 (*stars*), M33 (*squares*), and the Fornax dwarf galaxy (*pentagons*) are also shown. ωCen and M31 G1 are shown as an emphasized cross and star, respectively. NGC 5128 clusters with possible extratidal light are marked with partly filled circles.

galaxies overlap much more closely with Galactic globular clusters than those in NGC 5128. This is because κ_2 is dominated by the mean surface brightness within the effective radius and the NGC 5128 clusters are on average lower in mean surface brightness within this radius (e.g. see Figure 7).

While the NGC 5128 globular clusters overlap more with other globular clusters than galaxies, they are an even better match to the nuclei of the dwarf ellipticals studied by Geha et al. (2002), who measured both integrated and nuclear velocity dispersions and surface brightnesses for a sample of Virgo dwarf ellipticals. While the integrated properties of nucleated dwarf galaxies (*large, open squares*) fall within the region of κ–space inhabited by other dwarf ellipticals and spheroids (*diamonds*), their nuclei (*squares with crosses*) overlap very well with the NGC 5128 clusters.

The $\kappa_1-\kappa_2$ relation for giant elliptical galaxies and bulges exhibits an anticorrelation between mass and surface brightness that sets them nearly orthogonal to the dwarf galaxies, which are correlated in $\kappa_1-\kappa_2$. This correlation reflects the correlation between luminosity and larger cores of higher surface brightness found by Kormendy (1985). While this correlation suggests mass loss due to winds, Bender et al. (1992) found that mass loss would produce too steep a relation between κ_1 and κ_2, instead suggesting the observed dwarfs are the remnants of a larger, unobserved population. The massive globular clusters appear to exhibit a similar $\kappa_1-\kappa_2$ correlation, although steeper than the dwarf galaxies.

7. DISCUSSION

The strong dynamical and photometric similarities of these massive globular clusters to the nuclei of dwarf galaxies has interesting implications for models which posit stripped dwarf galaxy nuclei as the origin of the most massive globular clusters. The most massive Local Group clusters, such as ωCen in our own Galaxy and G1 in M31, have both been discussed and modeled as stripped dwarf nuclei (Freeman 1993; Meylan et al. 2001; Gnedin et al. 2002; Bekki & Freeman 2003). The position of ωCen and G1 in Figures 7 and 9 show that the NGC 5128 clusters occupy a similar region of the fundamental plane and κ–space. All of these massive clusters have comparable masses, mass-to-light ratios, and central surface brightnesses.

Support of the interpretation of these clusters as tidally-stripped galaxy nuclei is provided by the tentative detection of extratidal light by Harris et al. (2002) for six of the globular clusters (marked with an *x* in Table 2 and 3, *partly filled circles* in the figures). In the context of the stripped-dwarf model, it is tempting to view this extratidal light as the last vestiges of the extended dwarf envelope around these nuclei, although extratidal light may also be present due to the evaporation of cluster stars by two-body relaxation. Deeper observations of these and other massive clusters would be extremely valuable to confirm and quantify this extratidal light. Such observations would also better quantify the ellipticities of these globular clusters, which are comparable to those of ωCen and G1 but greater than those of dwarf nuclei.

These globular clusters may also simply represent the upper end of the globular cluster mass function in NGC 5128. The similarities between these globular clusters and the most massive globular clusters in the Local Group are more established than the interpretation of the better-studied Local Group clusters as tidally-stripped dwarf nuclei. In addition, there is evidence for yet more massive young star clusters that demonstrate that there is overlap between the masses of the most massive star clusters and the least massive dwarf galaxies. The most massive star cluster known is W3, a cluster with $\sigma = 45$ km s^{-1} in the merger remnant NGC 7252 (Maraston et al. 2004). The inferred mass of this cluster is nearly 10^8 $M_\odot$, even more massive than the nuclei of the dwarf galaxies studied by Geha et al. (2002). Even if we were to make the extreme suggestion that all of the NGC 5128 globular clusters are in fact relic dwarf nuclei, the existence of W3 demonstrates there is overlap between the masses of galaxies and star clusters.

On the other side of the mass gap, the ultra-compact dwarf galaxies in the Fornax cluster (Drinkwater et al. 2003) are actually *less* massive than W3 and overlap with the most massive NGC 5128 clusters. These dwarfs have velocity dispersions of $\sigma = 24-37$ km s^{-1}, effective radii of 10 – 30 pc, masses in the range 10^{7-8} $M_\odot$, and mass-to-light ratios of 2 – 4 in solar units (Drinkwater et al. 2003). They are thus very comparable to the larger and more massive of the NGC 5128 globular clusters. Numerical models for these ultra-compact dwarfs have shown that they can form from nucleated dwarfs that have been stripped of their envelopes by tidal forces in a cluster (Bekki et al. 2003). This stripping process can explain the ultra-compact dwarfs in Fornax, although it will operate over approximately a factor of 2 smaller radius in a smaller group like NGC 5128 due to decreased tidal shear. The radius for the tidal stripping of NGC 5128 globular cluster progenitors is likely to be on order 10 kpc (Bekki et al. 2003, see their Figure 7), comparable to the projected distances of 5 – 23 kpc for some of the NGC 5128 globular clusters in this study. It is therefore plausible that tidal stripping could have transformed at least some nucleated dwarf galaxies into these NGC 5128 globular clusters.

Another aspect of the tidally-stripped dwarf model is that their dark matter halos cannot be too cuspy as otherwise the

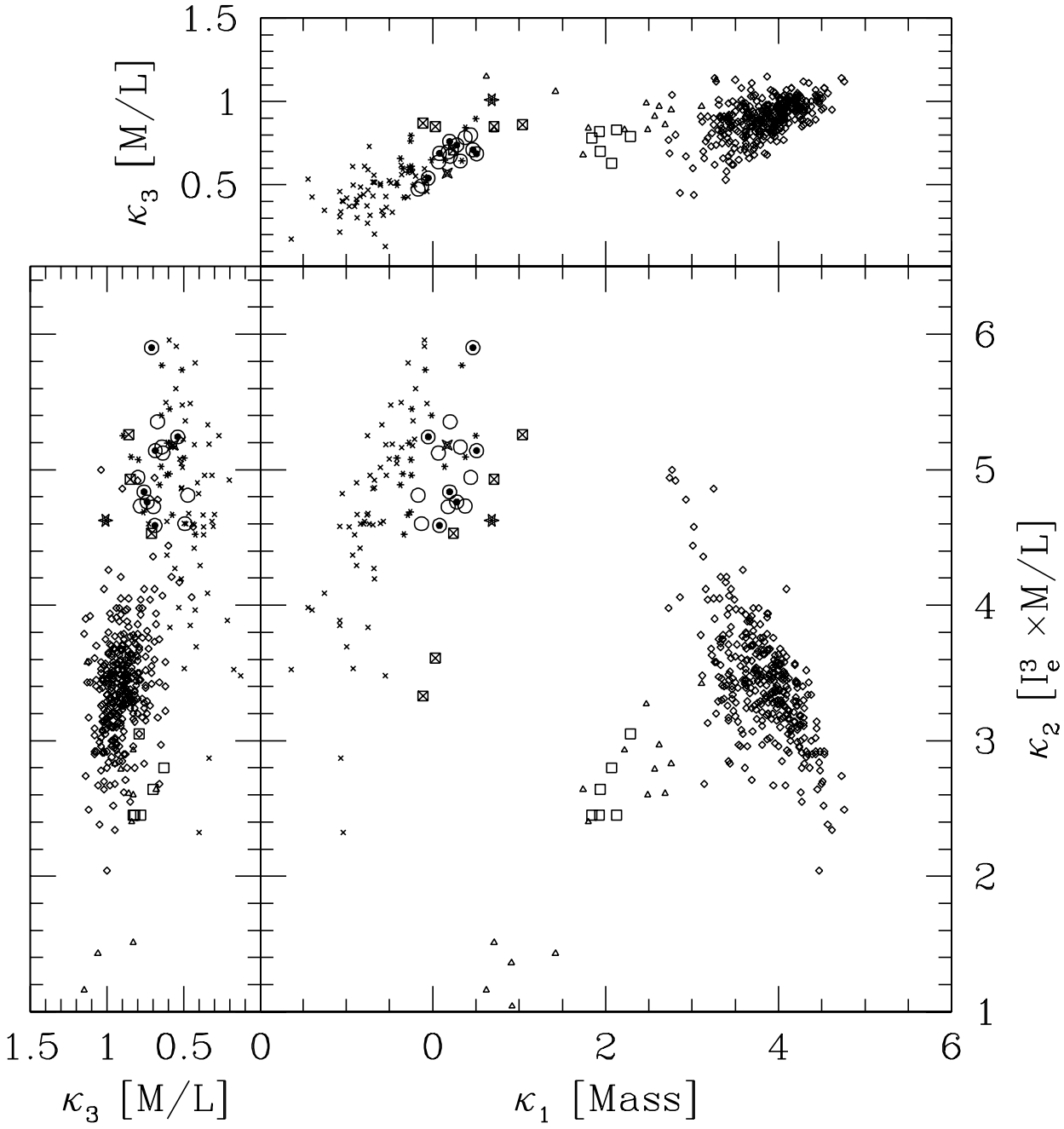

FIG. 9.—Projections of 3-dimensional κ–space. The NGC 5128 globular clusters (*open, large circles*, or *partly filled circles* for those with possible extratidal light) are in the region of κ–space that overlaps the most massive Galactic globular clusters (*crosses*), M31 clusters (*stars*) and dE nuclei (*squares with crosses*). ωCen and M31 G1 are shown as an emphasized cross and star, respectively. The integrated properties of the dEs (*open squares*) place them among other dEs and dSphs (*open triangles*). Elliptical galaxies and bulges are also shown (*diamonds*).

relatively concentrated dark matter core will be too effective at retaining the stellar envelope. In their study, Bekki et al. (2003) used the dark matter profile of Salucci & Burkert (2000) (originally proposed by Burkert (1995) for dwarf galaxies), rather than the more commonly adopted profile of Navarro, Frenk, & White (1996), because it has a flatter core. However, this requirement for a relatively flat dark matter core may remove one possible explanation for the higher mass-to-light ratio of these massive globular clusters. While a residual dark matter halo from their dwarf galaxy past is a possible explanation for the larger mass-to-light ratios of these NGC 5128 clusters, a dark matter profile with a flat, low-density core will also be more efficiently stripped away (Bekki et al. 2003). An alternative explanation for the high mass-to-light ratios of these massive globular clusters is if they formed in a starburst with a truncated stellar initial mass function (Charlot et al. 1993). A mass function with relatively more low-mass stars would produce a higher mass-to-light ra-

tio.

The detailed shapes and kinematics of the nuclei of nucleated dwarfs and the most massive globular clusters may provide one way to further investigate the potential connection between these two populations. The most massive globular clusters have significant ellipticities (Harris et al. 2002), while this does not appear to be the case for the nuclei of nucleated dwarfs (Geha et al. 2002). However, the same tidal forces that strip a dwarf envelope may also induce significant ellipticities. The importance of rotational flattening and anisotropies in the velocity distribution may also serve to distinguish between dwarf nuclei and globular clusters.

The hypothesis that some of the most massive globular clusters are the nuclei of galaxies offers an appealing explanation for recent evidence of an intermediate-mass black hole in G1 (Gebhardt, Rich, & Ho 2002). The mass of this black hole falls on the same $M_{BH} - \sigma$ relationship for galaxies and suggests that the formation mechanisms for black holes in star clusters and galaxy spheroids are similar. If G1 is instead simply a tidally-stripped, nucleated dwarf galaxy, the problem is reduced in complexity and only one physical mechanism for black hole growth is required to explain the $M_{BH} - \sigma$ relation.

An alternate interpretation of the similarity between the most massive globular clusters and the nuclei of nucleated dwarfs is that the later are simply star clusters that have migrated to or formed at the centers of these dwarfs. The properties of these objects would then be probes of massive star clusters in different environments, rather than of actual overlap between the properties of the most massive star clusters and the least massive galaxies. This interpretation also explains their similar location in κ–space, although stands in contrast to the simple explanation for the intermediate-mass black hole in G1.

8. SUMMARY

We have measured velocity dispersions for a sample of 14 globular clusters in the nearby, luminous elliptical galaxy NGC 5128, the first such study of the globular cluster system of a luminous elliptical galaxy and the first such study outside the Local Group. These clusters have velocity dispersions in the range 10 – 30 km s^{-1}, comparable to the largest previously measured values for globular clusters. We have used measured King model structural parameters for these clusters from the literature to derive masses for all 14 clusters. These clusters are comparable in mass to the most massive Galactic globular cluster ωCen and M31's G1. From these data we find the following:

1. The globular clusters in NGC 5128 approximately follow the same fundamental plane relationships as Local Group globular clusters and extend them to approximately an order of magnitude higher mass and luminosity.
2. The mean mass-to-light ratio of these clusters is larger than for typical Local Group globular clusters, although comparable to the more massive Local Group clusters.
3. These clusters begin to bridge the mass gap between the most massive globular clusters and the least massive dwarf galaxies. In particular, there is very good overlap in the photometric, structural, and kinematic properties of these clusters and the properties of both nucleated dwarf elliptical nuclei and ultra-compact dwarf galaxies.
4. The large masses of these clusters, combined with the possible detection of extratidal light for some objects by Harris et al. (2002), suggest that some of these globular clusters are in fact the nuclei of tidally stripped dwarf galaxies.

The common properties of the most massive star clusters and the nuclei of the least massive dwarfs suggest that both the formation mechanisms for star cluster and galaxies can produce objects in the same region of the fundamental plane or κ–space. Alternately, the nuclei of nucleated dwarf galaxies may simply be star clusters that happen to lie in the centers of galaxies, rather than true galaxy nuclei. Future spectroscopic observations of additional massive globular clusters could quantify the relative contribution of relic dwarf nuclei to this population through kinematics and with stellar population models, while deep, high-resolution images could provide better measurements of structural parameters, particularly in the core, and search for and study diffuse, low surface-brightness envelopes.

We would like to thank the staff of Las Campanas Observatory for their excellent support, in particular for making the MIKE spectrograph available after domestic security concerns delayed PANIC. We acknowledge useful discussions with Dan Kelson and thank Francois Schweizer, John Huchra, and the referee for helpful comments on the manuscript. PM received support from a Carnegie Starr Fellowship and a Clay Fellowship. The research of LCH is supported by the Carnegie Institution of Washington and by NASA grants from the Space Telescope Science Institute (operated by AURA, Inc., under NASA contract NAS5-26555).

REFERENCES

Ashman, K. M., & Zepf, S. E. 1992, ApJ, 384, 50
Barmby, P., Holland, S., & Huchra, J. P. 2002, AJ, 123, 1937
Barth, A. J., Ho, L. C., & Sargent, W. L. W. 2002, AJ, 124, 2607
Bassino, L. P., Muzzio, J. C., & Rabolli, M. 1994, ApJ, 431, 634
Battistini, P., Bonoli, F., Pecci, F. F., Buonanno, R., & Corsi, C. E. 1982, A&A, 113, 39
Bekki, K., Couch, W. J., Drinkwater, M. J., & Shioya, Y. 2003, MNRAS, 344, 399
Bekki, K. & Freeman, K. C. 2003, MNRAS, 346, L11
Bender, R., Burstein, D., & Faber, S. M. 1992, ApJ, 399, 462
Bendinelli, O., et al. 1993, ApJ, 409, L17
Bernstein, R., Shectman, S. A., Gunnels, S. M., Mochnacki, S., & Athey, A. E. 2003, Proc. SPIE, 4841, 1694
Binney, J., & Tremaine, S. 1987, Galactic Dynamics (Princeton, NJ, Princeton University Press)
Burkert, A. 1995, ApJ, 447, L25
Burstein, D., Bender, R., Faber, S., & Nolthenius, R. 1997, AJ, 114, 1365
Charlot, S., Ferrari, F., Mathews, G. J., & Silk, J. 1993, ApJ, 419, L57
Côté, P., Marzke, R. O., & West, M. J. 1998, ApJ, 501, 554
Crampton, D., Cowley, A. P., Schade, D., & Chayer, P. 1985, ApJ, 288, 494
Djorgovski, S. 1995, ApJ, 438, L29
Djorgovski, S., & Davis, M. 1987, ApJ, 313, 59
Djorgovski, S. G., Gal, R. R., McCarthy, J. K., Cohen, J. G., de Carvalho, R. R., Meylan, G., Bendinelli, O., & Parmeggiani, G. 1997, ApJ, 474, L19
Dressler, A., Lynden-Bell, D., Burstein, D., Davies, R. L., Faber, S. M., Terlevich, R., & Wegner, G. 1987, ApJ, 313, 42
Drinkwater, M. J., Gregg, M. D., Hilker, M., Bekki, K., Couch, W. J., Ferguson, H. C., Jones, J. B., & Phillipps, S. 2003, Nature, 423, 519
Dubath, P., & Grillmair, C. J. 1997, A&A, 321, 379
Dubath, P., Meylan, G., & Mayor, M. 1992, ApJ, 400, 510
—. 1997, A&A, 324, 505
Forbes, D. A., Brodie, J. P., & Grillmair, C. J. 1997, AJ, 113, 1652
Freeman, K. C. 1993, in ASP Conf. Ser. 48: The Globular Cluster-Galaxy Connection, 608
Fusi Pecci, F., et al. 1994, A&A, 284, 349
Gebhardt, K., Rich, R. M., & Ho, L. C. 2002, ApJ, 578, L41
Geha, M., Guhathakurta, P., & van der Marel, R. P. 2002, AJ, 124, 3073

Gnedin, O. Y., Zhao, H., Pringle, J. E., Fall, S. M., Livio, M., & Meylan, G. 2002, ApJ, 568, L23
Grillmair, C. J., Ajhar, E. A., Faber, S. M., Baum, W. A., Holtzman, J. A., Lauer, T. R., Lynds, C. R., & O'Neil, E. J. 1996, AJ, 111, 2293
Harris, G. L. H., Hesser, J. E., Harris, H. C., & Curry, P. J. 1984, ApJ, 287, 175
Harris, W. E. 1996, AJ, 112, 1487
Harris, W. E., Harris, G. L. H., Holland, S. T., & McLaughlin, D. E. 2002, AJ, 124, 1435
Heasley, J. N., Friel, E. D., Christian, C. A., & Janes, K. A. 1988, AJ, 96, 1312
Held, E. V., Federici, L., Testa, V., & Cacciari, C. 1997, in ASP Conf. Ser. 116: The Nature of Elliptical Galaxies; 2nd Stromlo Symposium, 500
Illingworth, G. 1976, ApJ, 204, 73
Israel, F. P. 1998, A&A Rev., 8, 237
Kaviraj, S., Ferreras, I., Yoon, S., & Yi, S. K. 2004, MNRAS, *submitted* (astro-ph/0402079)
Kelson, D. D. 2003, PASP, 115, 688
Kelson, D. D., Illingworth, G. D., van Dokkum, P. G., & Franx, M. 2000, ApJ, 531, 184
King, I. R. 1966, AJ, 71, 64
Kormendy, J. 1985, ApJ, 295, 73
Kundu, A., & Whitmore, B. C. 2001, AJ, 121, 2950
Kurtz, M. J., & Mink, D. J. 1998, PASP, 110, 934
Larsen, S. S., Brodie, J. P., Huchra, J. P., Forbes, D. A., & Grillmair, C. J. 2001, AJ, 121, 2974
Larsen, S. S., Brodie, J. P., Sarajedini, A., & Huchra, J. P. 2002, AJ, 124, 2615
Mackey, A. D., & Gilmore, G. F. 2003, MNRAS, 340, 175
Magorrian, J., et al. 1998, AJ, 115, 2285
Maraston, C., Bastian, N., Saglia, R. P., Kissler-Patig, M., Schweizer, F., & Goudfrooij, P. 2004, A&A, *in press*
McLaughlin, D. E. 2000, ApJ, 539, 618
Meylan, G., Mayor, M., Duquennoy, A., & Dubath, P. 1995, A&A, 303, 761
Meylan, G., Sarajedini, A., Jablonka, P., Djorgovski, S. G., Bridges, T., & Rich, R. M. 2001, AJ, 122, 830
Navarro, J. F., Frenk, C. S., & White, S. D. M. 1996, ApJ, 462, 563
—. 2004, ApJS, 150, 367
Peng, E. W., Ford, H. C., & Freeman, K. C. 2004, ApJ, *in press*
Pryor, C., & Meylan, G. 1993, in ASP Conf. Ser. 50: Structure and Dynamics of Globular Clusters, 357
Rejkuba, M. 2004, A&A, 413, 903
Rich, R. M., Mighell, K. J., Freedman, W. L., & Neill, J. D. 1996, AJ, 111, 768
Richstone, D. O., & Tremaine, S. 1986, AJ, 92, 72
Rix, H., & White, S. D. M. 1992, MNRAS, 254, 389
Salucci, P., & Burkert, A. 2000, ApJ, 537, L9
Sarajedini, A., Geisler, D., Harding, P., & Schommer, R. 1998, ApJ, 508, L37
Schweizer, F. 1987, in Nearly Normal Galaxies. From the Planck Time to the Present, 18–25
Tonry, J. & Davis, M. 1979, AJ, 84, 1511
van der Marel, R. P. 1991, MNRAS, 253, 710
Yi, S. K., Peng, E., Ford, H., Kaviraj, S., & Yoon, S. . 2004, MNRAS, *in press* (astro-ph/0401454)
Zinnecker, H., Keable, C. J., Dunlop, J. S., Cannon, R. D., & Griffiths, W. K. 1988, in IAU Symp. 126: The Harlow-Shapley Symposium on Globular Cluster Systems in Galaxies, 603